

Article

Hydrodynamic and Sediment Transport Patterns in the Minho and Douro Estuaries (NW Portugal) Based on ADCP Monitoring Data: Part 2—Statistical Interpretation of Bottom Moored Datasets

Ana Isabel Santos ^{1,*}, Anabela Oliveira ¹, Dora Carinhas ¹, José Paulo Pinto ¹ and M. Conceição Freitas ^{2,3}

¹ Instituto Hidrográfico, Rua das Trinas 49, 1249-093 Lisboa, Portugal; anabela.oliveira@hidrografico.pt (A.O.); dora.carinhas@hidrografico.pt (D.C.); paulo.pinto@hidrografico.pt (J.P.P.)

² Departamento de Geologia, Faculdade de Ciências da Universidade de Lisboa, Campo Grande, 1749-016 Lisboa, Portugal; cfreitas@fc.ul.pt

³ Instituto Dom Luiz, Faculdade de Ciências da Universidade de Lisboa, Campo Grande, 1749-016 Lisboa, Portugal

* Correspondence: ana.santos@hidrografico.pt

Abstract: Exploratory statistical partitioning methods (K-means Clustering analysis) were applied to ADCP monitoring datasets collected inside the Douro and Minho estuaries. This analysis is aimed to discriminate ADCP acoustic responses according to the variations of the suspended particles within the ensonified medium. Based on the interpretation of the results, this work establishes general sediment transport patterns at both estuaries' exits under continuously varying river flows and tidal amplitudes recorded during a summer dry seasonal scenario (September 2005) and winter high river discharge (January/February 2007) conditions. Results confirm the already known present scarcity of (sandy) sediment export from the Douro and Minho estuaries into the inner shelf and the consequent sediment depletion of the adjacent littoral, with no effective contribution of the Douro and some evidence of sand export observed at the Minho outlet during the winter of 2007.

Keywords: estuarine dynamics; sediment transfer; acoustic backscatter; Minho; Douro



Citation: Santos, A.I.; Oliveira, A.; Carinhas, D.; Pinto, J.P.; Freitas, M.C. Hydrodynamic and Sediment Transport Patterns in the Minho and Douro Estuaries (NW Portugal) Based on ADCP Monitoring Data: Part 2—Statistical Interpretation of Bottom Moored Datasets. *Coasts* **2021**, *1*, 56–72. <https://doi.org/10.3390/coasts1010004>

Academic Editor: Athanassios A. Dimas

Received: 29 September 2021
Accepted: 16 November 2021
Published: 20 November 2021

Publisher's Note: MDPI stays neutral with regard to jurisdictional claims in published maps and institutional affiliations.



Copyright: © 2021 by the authors. Licensee MDPI, Basel, Switzerland. This article is an open access article distributed under the terms and conditions of the Creative Commons Attribution (CC BY) license (<https://creativecommons.org/licenses/by/4.0/>).

1. Introduction

In the Portuguese coastal zone, sea level stabilization took place ≈ 3500 years BP. Since then, the general atmospheric patterns, potentiated by the increase on human activities had a significant effect on the increase of sediment supply, resulting on an overall sediment infill of estuaries, lagoons and gulfs. However, by the end of the XIX century, this scenario dramatically changed and the Portuguese littoral gained a regressive trend, with the first reports of “sea invasions” [1]. This regressive behavior is related with the sediment supply reduction due to human intervention, namely, the damming of rivers; sand extraction; new agricultural practices aiming soil conservation and construction of coastal engineering structures [1,2]. Presently, sediment transfer estimates report that the sediment budget in the Portuguese northern coastal cells has radically changed, mainly due to the reduction of the fluvial input, revealing a severe sediment deficit, followed by an accentuated erosive tendency in some segments of the coast [2–4].

Under these circumstances, the quantification of the present effective sediment exchanges between the northern Portuguese estuaries and the inner continental shelf and coastal zone is crucial to establish the scenario of the consequent implications and the design of urgent coastal management actions. In order to address this problem, the implementation of pragmatic monitoring solutions and the compilation of previously collected data has become a priority in order to establish the present sediment dynamic regime in this area.

In the past, several long-term datasets of Acoustic Doppler Current Profilers (ADCP) were collected at diverse locations in the Portuguese inner shelf, coastal zone and estuaries, covering different seasonal regimes. These datasets, with different objectives or scientific projects in mind, were processed and interpreted to establish the hydrodynamic regime in their respective study areas, but no attempt was made to establish sediment transport patterns for the duration of their deployment.

From the years 2005–2008, Project ECOIS (Estuarine Contributions to Inner Shelf Dynamics) aimed to evaluate the way that the Douro and Minho river discharge variations induced changes in estuarine dynamics and, consequently, in the sediment transfer rates between the estuaries and the inner continental shelf and coastal zone. During this project, ADCP datasets were collected near the outlets (“Barra”) of the Douro and Minho estuaries in the summer of 2005 and the winter of 2007, covering contrasting seasonal forcing regimes and with time series spanning continuously under neap and spring tide conditions.

According to Santos et al. (2021) [5], hereafter referred as Part 1 of this study, field data collected during ECOIS revealed that under spring tide/low runoff conditions, the Minho estuary effectively imports sediments from the inner shelf with suspended material entering the estuary via flood current at near bottom levels. When river discharge levels increase and during neaps, the Minho estuary effectively exported sediments into the inner shelf, in the order of 10^5 kg of sediments per tidal cycle measured at a point near the river mouth. Part 1 also revealed that evidence of sediment export exists in the Douro estuary, when Crestuma Dam discharges exceed $500 \text{ m}^3/\text{s}$ also during neaps, with calculated sediment export values for the winter of 2006 neap tide observations in the order of 10^5 kg per semi-diurnal tidal cycle. When the tidal amplitude is high (spring tide) and there is no significant discharge, there is some sediment import associated with near bottom flood currents that remobilize and transport bottom material upstream. During the winter of 2006 survey, the effective water and sediment export into the inner shelf by both estuaries was corroborated by data collected in the inner shelf during the same period [6].

Although there is sufficient data to evidence sediment and water export during high runoff/neap tide events (see Part 1), questions remain about the nature (particle size) and fate of these sediments when they reach the inner shelf. According to the conceptual model presented by Alveirinho Dias et al. (2002), most sediment reaches the shelf via flood discharges (high river runoff events) from fluvial systems such as the Douro and Minho, with negligible export from the Galician Rias. During periods of stormy weather, and consequent downwelling situations, swells predominantly coming from the NW transport the fines to the mid-outer shelf, and the sands are only remobilized during the most extreme wave conditions. If rivers effectively transport some coarser sediments (mainly sands), these can, eventually, be incorporated into the littoral drift and nourish the sediment depleted coastal zone [7].

ADCP acoustic backscatter data has been used to estimate particle concentration and size in various environments. Among many, early attempts were made using sediment acoustic systems by Libicki et al. (1989) [8] in the deep ocean and by Hanes et al. (1988) [9] in the shallow nearshore zone following the concepts described by Hay (1983) [10]. With the widespread use of commercial ADCPs operating typically at 200–1200 kHz, the interest in extracting suspended sediment concentration and grain size from the backscatter signal strength grew, with several authors presenting promising results (e.g., [11,12] in coastal environments; [13–17] to measure sand and silt in large rivers, among many others).

Santos et al. (2020) established a methodology to extract indicative mean grain size from single-frequency ADCP monitoring data [18], coupled with concurrent sediment concentration measurements based on LISST technology (Laser in-situ transmissometry [19,20]). Unfortunately, at the time of the ECOIS field surveys, LISST technology, which would be able to provide both concentration and particle size measurements, was still being implemented so no LISST data is available for the time of the discussed ADCP deployments. In addition, during the ECOIS field surveys, no sufficient water sampling concentration values were

available to calibrate the acoustic backscatter records of the bottom moored ADCP's, which invalidates the methodology presented by these authors.

In a further attempt to extract suspended sediment information from single frequency ADCP monitoring data, and assuming that the acoustic metrics of acoustic backscatter and attenuation relate to suspended particle concentration and size, Santos et al. (2021) considered that different suspended sediment signatures in terms of concentration and particle size yield statistically different ADCP acoustic responses [21]. To this end, commonly used exploratory statistical tools were applied to cluster the ADCP's acoustic response into statistically significant different groups or populations. The resulting ADCP clusters were then characterized in terms of suspended sediment concentrations and particle size distribution based on concurrent LISST measurements, revealing three distinct suspended particle populations, with the same general characterization in all analyzed datasets collected at three distinct locations in the Portuguese coastal shelf.

In the present work, the clustering methods presented in [21] will be applied to the ECOIS monitoring datasets in an attempt to interpret the ADCP's acoustic response to the particles within the ensonified medium of the Minho and Douro estuarine water column, taking into account the contrasting forcing scenarios at the time of the deployments.

As its final objective, this work and Part 1 of this study, aim to establish the general sediment transport patterns at both estuaries' exits under continuously varying river flows and tidal amplitudes recorded during an end of summer dry seasonal scenario and winter high river discharge conditions.

2. Materials and Methods

2.1. Field Work and Data Collection

Under the scope of ECOIS, two hydro-sedimentological field surveys were carried out in September 2005 and January/February 2007 (see Table 1). During these surveys, bottom moored ADCP's were deployed to provide continuous time series of pressure, temperature, current structure (magnitude and direction) and acoustic backscatter in an attempt to extend observations for periods longer than a two-week fortnightly tidal cycle. In the scope of the same field surveys, intensive sampling programs inside both estuaries were carried out during spring and neap tide periods. Some of these results are discussed in Part 1 of this study. Figure 1 summarizes the location of the deployments in both estuaries, which were approximately the same for all surveys, and Table 1 resumes the field configurations of the four ADCP datasets discussed in this work. In both cases, the Barra ("outlet") position is representative of the estuaries' lower end. A detailed description of the study area is provided in Part 1 of this study. ADCP's (RDI Workhorse Sentinel) were deployed using bottom fixed mooring structures, with the ADCP's in an up-looking position, covering the whole estuary water column from 1 to 2 m above bottom up to the surface. Near the bottom, and using the same mooring structure, an additional Anderaa RCM9 point current meter was deployed with additional sensors of salinity, temperature and turbidity, in an attempt to cover the current and hydrological structure of the near bottom layer, not covered by the ADCP readings. Salinity or temperature datasets recorded by these auxiliary current meters will be used in this work in the interpretation of the water column hydrological characteristics throughout the measuring periods. Turbidity data recorded by these same current meters was frequently not valid due to the scaling of the sensor and will be disregarded.

Table 1. ECOIS ADCP dataset information.

		Start	End	Sample Interval (min)	1st Bin (mab *)	Bin Size (m)	Freq. (kHz)	Hourly Samples
ECOIS 2005	Minho (Barra)	08-Sep-2005 11:42:30	15-Sep-2005 05:42:30	5	1.61	0.5	600	163
	Douro (Barra)	10-Sep-2005 07:28:23	01-Oct-2005 07:28:23	5	1.61	0.5	600	505
ECOIS 2007	Minho (Barra)	17-Jan-2007 14:45:00	30-Jan-2007 20:45:00	10	1.61	0.5	600	319
	Douro (Barra)	20-Jan-2007 16:25:00	15-Feb-2007 13:25:00	10	1.61	0.5	600	622

* meters above bottom.

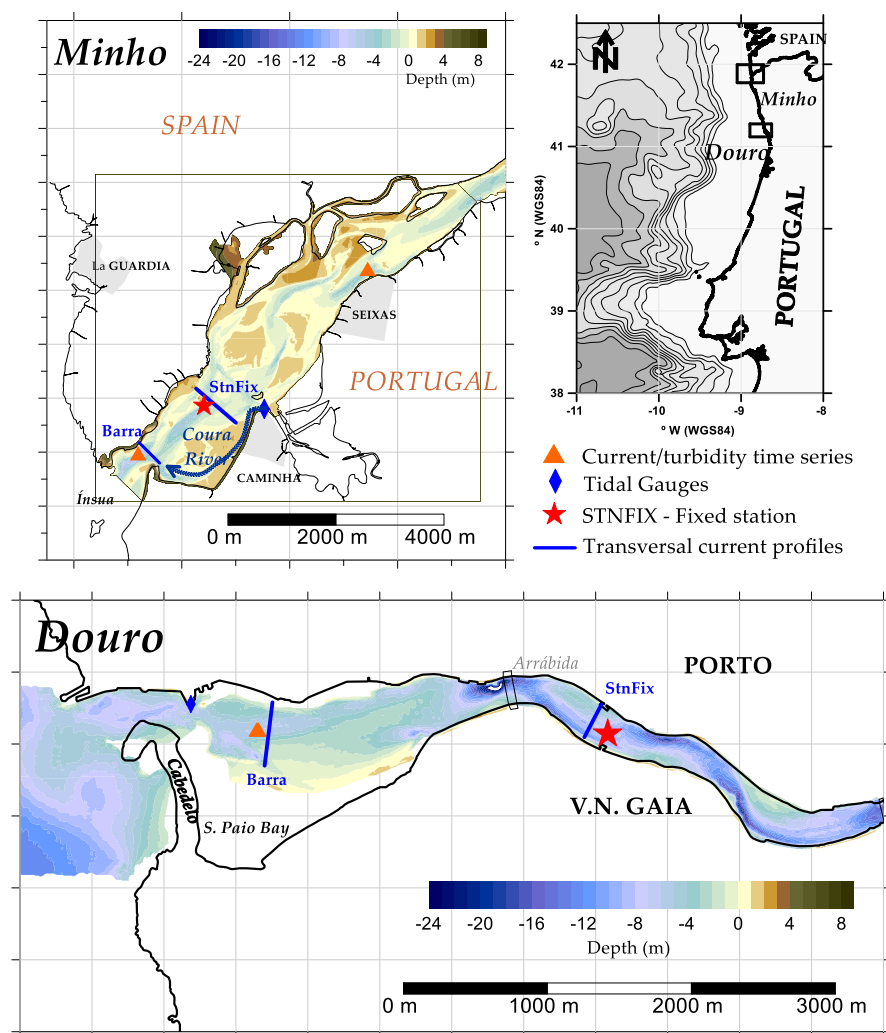


Figure 1. Location and summary of observations in the Minho and Douro estuaries, superimposed on the bathymetry data collected during ECOIS surveys [22].

Limited suspended sediment information is available for the ECOIS field surveys collected via water sampling and laboratory analysis (concentration and grain size). A more detailed account of these results is addressed in Part 1 of this study. Grain size analyses yielded modes that ranged from 0.01–0.02 mm (very fine to medium silt) in both estuaries, however, the laboratory protocol on these analyses involved both the chemical digestion of organic matter and the use of anti-flocculation agents. In estuarine environments,

such as the ones studied in this work, flocculation of clay material and organic matter transported by the river course in the presence of higher salinity values and turbulence is a key phenomenon conditioning the hydrodynamic behavior of the particles in the water column. A floc or aggregate may constitute an order of 10^6 individual particles and floc size can range over 4 orders of magnitude within any one floc population, from clay particles of 1 μm diameter to macroflocs of several millimeters [23,24]. Inside both the Minho and Douro estuaries, X-ray diffraction revealed a general mineralogical composition of mostly illite and kaolinite with high organic matter content [6], so it is very likely that the grain size actually in suspension inside the estuaries might in fact be much larger than the reported 0.01–0.02 mm, although, intrinsically, it is still fine material.

The development of a theoretical description of how acoustic systems interact with flocculating sediments has been lacking and this deficiency has impeded sound being used to extract quantitative suspended sediment parameters from ADCP acoustic backscatter in suspensions containing flocs [25]. However, Vincent and McDonald (2015) concluded that both acoustic (ADCP) and the optic (LISST) in-situ measurements were consistent with the scattering of the tightly bound flocculi as opposed to the larger flocs [23,26], and that these flocculi could be treated as particles with density and acoustic wave propagation speeds close to those of the primary particles. These important facts will have to be taken into consideration when interpreting the acoustic response of the ADCP's in terms of the type of particles present in the estuaries' water column.

2.2. Data Processing and Statistical Analysis

In a first step, ADCP datasets were processed and validated taking into account registered instrument position (pitch and roll) and validation (percent-good) variables. ADCP records which didn't meet the required quality standards were discarded and replaced with "NaN" ("not a number"). After validation, datasets were time averaged to obtain representative hourly samples of current magnitude, direction and acoustic response (echo intensity in counts). For reader's convenience, Table 2 briefly describes the variables discussed in this work.

Table 2. Description of discussed ADCP outputs and forcing variables.

		Description
ADCP outputs	FCB (dB)	ADCP fluid corrected backscatter, i.e., ADCP (I_{ADCP}) acoustic response converted into dB according to Gostiaux and Van Haren (2010), corrected for fluid sound absorption and geometrical spreading, where R is the range to the ensonified volume; Ψ is the near field correction coefficient and α_w is the sound attenuation due to the surrounding fluid [15,18,27,28]. $\text{FCB} = I_{\text{ADCP}} + 20R\Psi + 20e R\alpha_w$
	Horizontal Velocity (m/s)	Current magnitude measured along the N-S and E-W horizontal axes.
	Direction ($^\circ$)	Current direction (horizontal) in degrees from N (counterclockwise).
	Vertical Velocity (m/s)	Velocity measured along the water depth axis.
	Error ² (m^2/s^2)	The uncertainty of ADCP velocity measurements includes two kinds of error: random or short-term error and bias. Averaging single ping ADCP measurements reduces the random error but not bias, which is intrinsic of any instrumental determination. According to Gordon (1996), external error sources such as turbulence dominate external error sources in broadband ADCP's. In this work, the square of the recorded velocity error is used as a proxy of the turbulent kinetic energy present during the measurements [29].

Table 2. Cont.

	Description
Cluster Analysis	Classification of the ADCP measurement according to the K-means cluster partition, for $k = 3$ ($k =$ number of considered populations = 3), applied to the normalized $z_{\text{score}}(\text{FCB})$.
Depth (m)	ADCP depth measured at the transducer.
Bin depth (m)	Depth of the ADCP's vertical measuring cell (bin). Depth inside the water column.
Tau (τ) (N/m^2)	Bottom shear stress, taking into account the horizontal velocity magnitude at the first bin and type of bottom (sand/gravel), according to the formulations of Soulsby (1997) [30].
Diameter (mm)	Potentially removable/transportable particle diameter taking into account near bottom current velocity (1 m above bottom, or the ADCP's first measuring bin), according with the formulations of Soulsby (1997) [30].
Salinity (PSU)	Near bottom salinity (measured at the Anderaa RCM9 point current meter)
Other outputs	
Temperature ($^{\circ}\text{C}$)	Near bottom temperature (measured at the Anderaa RCM9 point current meter)
Q (m^3/s)	River flow

In order to remove scaling effects, and according to the methodology described by Santos et al. (2021) [21], normalization ($z_{\text{score}} = (X - \mu) / \sigma$, where X is the measured value; μ is the time-series mean and σ the time-series standard deviation) was applied to the ADCP acoustic response, corrected for fluid sound absorption and geometrical spreading (FCB—fluid corrected backscatter) in order to simplify some of the interpretation of the results. Normalized (z_{score}) variables vary between 1 (maxima) and -1 (minima), with close to mean values ≈ 0 .

As mentioned, acoustic intensity cluster populations were identified applying K-means cluster analysis to normalized (z -score) FCB datasets, for $k = 3$ (3 clusters/acoustic populations), according to the methodology presented by Santos et al. (2021) [21]. These authors, focusing on near bottom sediment transport patterns and down-looking ADCP datasets, applied cluster analysis on the time series of the variable $z_{\text{score}}(\text{FCB})$ for the ADCP's first bin (vertical measuring cell) at the same vertical level as the LISST probe. The resulting populations were then characterized in terms of suspended sediment parameters (concentration, mean grain size, and fine sediment content) based on concurrent LISST measurements. Three distinct populations were identified by the authors with similar characteristics in all analyzed datasets:

- Population I (“Higher Fine”), characterized by higher than average $z_{\text{score}}(\text{FCB})$ corresponding to matching LISST higher than average sediment concentrations, higher than average fine sediment content and lower than average mean grain size;
- Population II (“Lower Coarse”) characterized by lower than average $z_{\text{score}}(\text{FCB})$, corresponding to matching LISST lower than average sediment concentrations, lower than average fine sediment content and higher than average mean grain size; and,
- Population III (“Standard”) characterized by average $z_{\text{score}}(\text{FCB})$ response, corresponding to matching LISST average sediment concentrations, average mean grain diameters and average fine sediment content.

In this work a similar statistical analysis was applied to the $z_{\text{score}}(\text{FCB})$ datasets collected in the Minho and Douro estuaries, but this time extending to all bins (vertical measuring cells) in the estuaries' water column, with the exception of the shallowest bins in order to eliminate the acoustic effect of the water surface from the $z_{\text{score}}(\text{FCB})$ classification [15]. After separation, the identified ADCP $z_{\text{score}}(\text{FCB})$ clusters were subject to a simple statistical characterization via the mean and standard deviation of the non-transformed and normalized ADCP variables and classified according to their $z_{\text{score}}(\text{FCB})$ range as Population I “High” (mean $z_{\text{score}}(\text{FCB}) > 1$), Population II “Low” (mean $z_{\text{score}}(\text{FCB}) < -1$) and Population III “Standard” (mean $z_{\text{score}}(\text{FCB}) \approx 0$). Note that in this case the desig-

nations “Fine” and “Coarse” used by Santos et al. (2021) were not applied, given that in this case there are no concurrent sediment measurements that will enable the conclusive characterization of the acoustic populations in terms of size.

3. Results

ECOIS field surveys were planned spanning the three-year project duration, with the first “reference” survey carried out at the end of summer of 2005 under equinoctial spring/neap tidal conditions and expected low or absent river runoff conditions. The 2007 winter survey was carried out under the expectation of high river discharge conditions, typical of Iberian wet winters.

Historic annual river flow analysis for the Minho, based on Foz de Mouro [31] and Frieira [32] hydrometric records from the hydrological year of 1973/1974 up to 2013/2014, shows a maximum of 869.9 m³/s in 2000/2001, almost three fold the 40-year average value of 314.2 m³/s and seven times the minimum of 125.5 m³/s registered in 1975/76. Hydrometric data for the Douro was obtained for the Crestuma Dam (upper limit of the estuary [33]) for the hydrological years 1985/86 up to 2014/2015. Mean annual river flow values in the Douro are highly variable with a maximum value of ≈1500 m³/s in 2000/2001, one order of magnitude higher than the minimum of ≈150 m³/s in 1991/1992. Mean annual flow value is 480 m³/s for the whole time series.

In this context, the first two ECOIS hydrological years (2004/2005 and 2005/2006) were considered dry, with annual mean flows below the mean in both the Minho and Douro (in the order of 200 and 200–300 m³/s, respectively). The last 2006/2007 hydrological year presented an annual mean flow approximately 50% higher than the series’ mean in both rivers (410 m³/s for the Minho and 650 m³/s for the Douro).

Table 3 resumes the river flow history of the ECOIS hydrological years in order to contextualize the presented results. As mentioned, the 2005 low runoff reference survey was characterized by an exceptionally dry hydrological year. The ECOIS 2007 survey was characterized by a dry January nested between an otherwise wet winter and preceding an exceptionally wet summer.

Table 3. Mean monthly discharges measured at Crestuma (1-January-1986 to 31-August-2007) and Foz de Mouro (1973/1974 to 2006/2007), compared with the individually monthly values for 2004/2005, 2005/2006 and 2006/2007 ECOIS hydrological years. The months when the discussed field surveys took place are shaded in gray, above mean values are marked in blue and below mean values are marked in red.

	Douro (Crestuma)				Minho (Foz do Mouro)			
	Mean (m ³ /s)	2004/2005 (m ³ /s)	2005/2006 (m ³ /s)	2006/2007 (m ³ /s)	Mean (m ³ /s)	2004/2005 (m ³ /s)	2005/2006 (m ³ /s)	2006/2007 (m ³ /s)
Oct.	281.61	381.33	36.94	518.31	189.12	240.27	130.29	305.76
Nov.	516.35	455.30	191.08	1449.83	314.80	362.55	168.33	627.19
Dec.	928.59	337.24	356.11	1470.04	511.79	237.90	204.58	1089.61
Jan.	1071.87	189.37	250.44	434.18	595.46	215.33	244.79	400.44
Feb.	857.26	223.74	270.82	948.21	589.20	175.78	258.64	722.90
Mar.	747.19	219.03	767.21	920.29	457.53	162.49	689.03	669.35
Ap.	507.23	301.20	582.76	382.92	346.59	169.36	469.03	314.04
May	399.54	171.07	263.58	462.73	263.83	201.31	199.20	176.16
Jun.	269.07	109.21	166.89	359.00	189.21	162.29	115.35	182.74
Jul.	160.91	63.00	132.91	267.28	152.22	113.46	126.13	212.13
Aug.	99.90	46.45	73.60	207.85	118.17	90.80	75.29	130.36
Sep.	162.86	62.33	93.16	—	116.97	81.79	116.99	102.17

3.1. Reference Situation (September 2005)

In the Minho Estuary, river discharge values measured at Foz de Mouro during the observation period show a permanent base value of approximately 50–60 m³/s, interrupted by short (under or approximately 6 h long) irregular peaks in the order 100–200 m³/s (Figure 2H).

Current velocity values at this point of the estuary vary between 0–1.5 m³/s, with maxima felt during spring tide floods, confirming the observations of Reis (2008) which states that a clear asymmetry exists between flood and ebb in both neap and spring conditions inside the Minho estuary: ebb is longer and less intense than flood, revealing a flood dominated estuary [34]. Near bottom salinity values at the Barra measuring point are in the order of 32 PSU, decreasing to 26–28 PSU in low tide. The magnitude of the salinity oscillation is directly related with the tidal amplitude (Figure 2H). Current directions generally follow the estuary channel's orientation, with floods directed to the NE and ebbs directed to the SW. The current structure reveals a vertical homogenous water column with no significant evidence of shear (Figure 2B,C). Vertical velocities in the water column are generally directed downwards during floods, with maxima felt near the bottom, and during ebbs and low tides, less intense values are generally headed upwards. Water column turbulence maxima is associated with the end of ebb and low tide, at mid-column/surface levels, and in some cases during floods, at near bottom levels (Figure 2D,E).

The Minho Barra dataset reveals a continuous pattern of two events of maximum FCB values: the first extending through the whole water column during floods and a second moment at the end of ebb/low tide in which $z_{\text{score}}(\text{FCB})$ maxima are concentrated at near bottom levels. Both these maxima are identified by cluster analysis as Population I (“High”) and are synchronous with periods when near bottom current velocities (and implicitly in the remaining water column) are potentially able to transport bottom sediment main modes (Figure 2A,F,G). Population II “Low” is, with no exception, associated with high tides and the beginning of ebb.

Ebb associated $z_{\text{score}}(\text{FCB})$ maxima near the bottom are synchronous with upwards oriented vertical velocities and higher turbulence values throughout the water column, suggesting resuspension of near bottom material which is then transported downstream by the remaining ebb flux. On the other hand, flood associated maxima is characterized by more intense bottom directed vertical velocities and turbulence concentrated near the bottom which seem to indicate local deposition and transport of material (potentially coarse at maximum flood flux capacity) entering the estuary. The significance of this flood associated maximum is also dependent on the tidal amplitude, with more extensive and longer maxima associated with spring tide amplitudes and dividing into separate “nuclei” at lower tidal amplitudes (one near the surface and one at near bottom levels). Although both of these Population “High” nuclei associated with flood occur simultaneously, in a nearly vertically homogeneous water column (see Part 1), the fact that they flow at separate levels in the estuaries' water column suggests that they are different in nature, with the near surface maximum corresponding to lower density fine or organic material and the near bottom “nucleus” to coarser (sandy) material which is cyclically deposited and eroded from the estuary and inner shelf bottom.

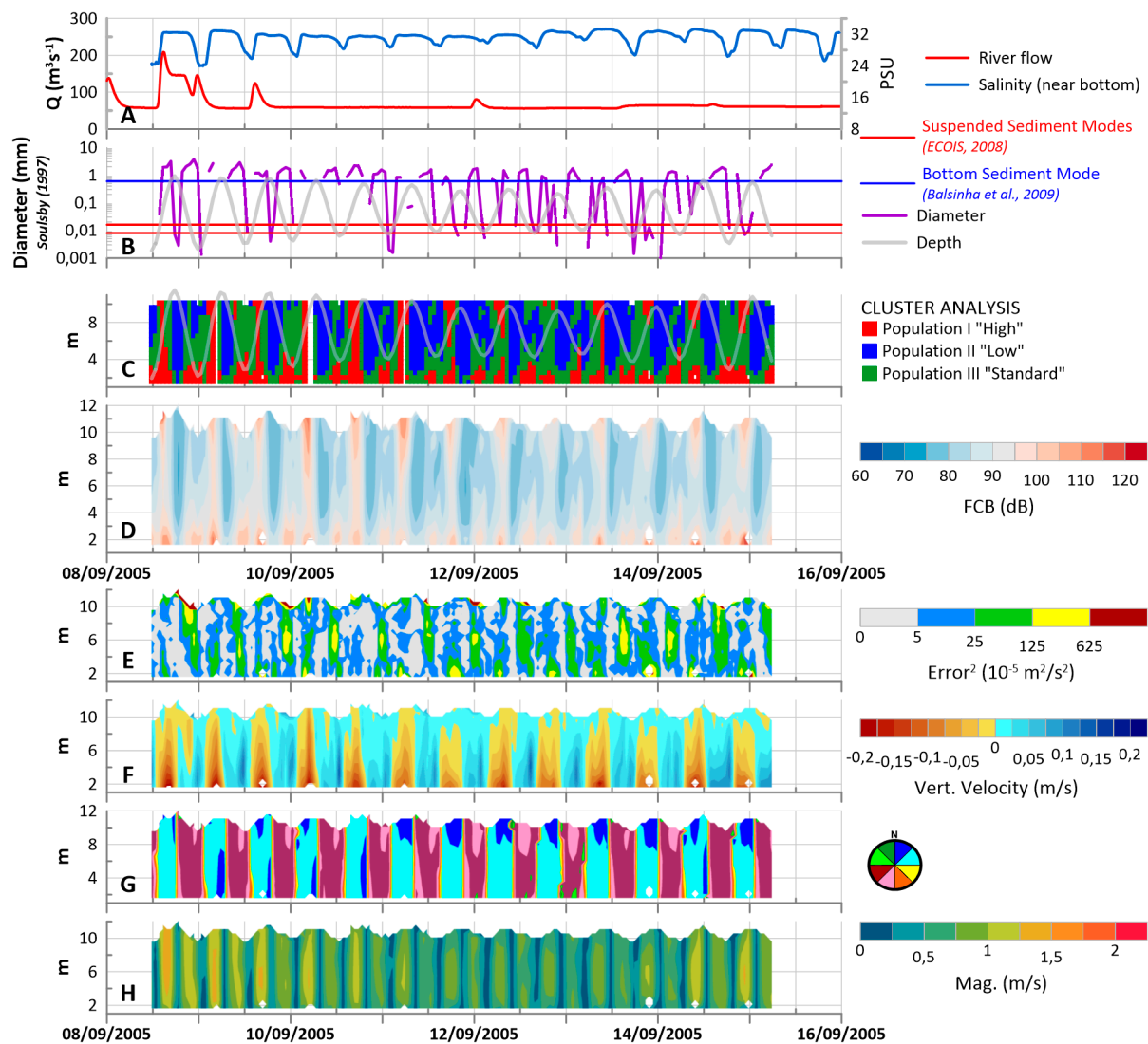


Figure 2. Minho 2005 “Barra” dataset. (A) Minho river flow measured at Foz de Mouro and near bottom salinity measured at the bottom mounted RCM9; (B) Potentially removable/transportable particle size [30] and known bottom sediment and suspended sediment main modes [22,35]; (C) K-means cluster analysis of $z_{score}(FCB)$ superimposed on ADCP transducer depth (tide); (D) Fluid Corrected backscatter (FCB); (E) error velocity squared (proxy of turbulent kinetic energy); (F) Vertical velocity; (G) Current direction; (H) Horizontal velocity (current magnitude).

For the same period, results presented in Part 1 identified the presence of higher sediment concentrations at the fixed station position (Figure 1) associated with spring low-tides, suggesting that there is still some sediment flowing from the upper estuary into the lower estuary even with near null river discharge. However, during neaps, clear suspended sediment maxima were always felt near the bottom during floods and no maxima were observed during ebbs at the fixed station, suggesting an upstream transport of suspended material coming in from the lower reaches of the estuary. Part 1 determined sediment exchange values between the estuary and the inner shelf in the order of 10^4 kg of sediment directed upstream (import) during a spring semi-diurnal tidal period and 10^3 kg of sediment directed downstream during neaps at the Barra position. According to our interpretation of the $z_{score}(FCB)$ cluster analysis, it is probable that the sediment import during spring tides results mainly on the cyclical remobilization of fine sand present at the estuary bottom and inner shelf by the tidal currents, which, in conjunction with the known Minho tidal asymmetry, yields a net import of sand into the lower estuary. However, during neaps, the separation of the flood associated $z_{score}(FCB)$ Population I

into two separate levels in the water column suggests that the net import of sediment into the estuary is consisted not only of coarse sandy material found at the estuary bottom, but also of some sort of lower density fine or organic material coming in from the ocean. Unfortunately, the exact origin or composition of these particles cannot be inferred from this dataset.

During the 2005 summer reference survey observation period, Crestuma Dam discharges into the Douro estuary were highly irregular, with null discharges during most of the observation period, interrupted by short term (<6 h) discharge peaks that reached as high as 750 m³/s. ADCP data collected at the Douro outlet (Barra) during this period confirm the results presented in Part 1. The estuary's water column presents an alternate vertically homogeneous structure during springs and vertical stratification during neaps, with ebbs mainly at the surface levels and floods at near bottom levels (Figure 3B,C). Both error² and vertical velocity measurements at this point of the Douro estuary reveal that, when compared with the Minho dataset, the Douro presents a stable water column with almost no evidence of turbulent phenomena (Figure 3D,E). Near bottom salinity oscillates with semi-diurnal tide between maxima of ≈36 PSU and minima of 28–30 PSU. The magnitude of the salinity oscillation depends on both the tidal amplitude and on Crestuma Dam discharges, with full series minima of ≈26 PSU registered at the Barra position immediately following a Crestuma discharge maximum > 600 m³/s (on 21 September 2005, see Figure 3H). $z_{\text{score}}(\text{FCB})$ maxima associated with low tide and beginning of the entering flood are felt throughout the whole dataset, classified as Population I "High" near the bottom and Population III "Standard" as the maxima subside towards the surface and as the flood progresses in time. $z_{\text{score}}(\text{FCB})$ minima (Population II "Low") are always associated with high-tides and most of the ebbs at near surface levels (Figure 3F). The observed $z_{\text{score}}(\text{FCB})$ cluster population pattern at this point of the estuary is in agreement with the conceptual model presented by Portela (2008) and Instituto Hidrográfico (1995), which concluded that suspended sediments, probably transported from the upper reaches of the Douro estuary, are transported by ebb currents in the surface layers towards the sea, and are "captured" by the flood currents in deeper levels of the water column, forming a "closed circulation" cell [36,37]. Results presented in Part 1 for this same survey period revealed the existence of sediment import into the estuary at the Barra site during both spring and neaps (in the order of 10⁴ kg per semi-diurnal tidal cycle). According to the formulations of Soulsby (1997) [30], bottom velocity magnitudes at the deployment site are very seldom able to remobilize local coarse bottom sediments, however, the same currents are able to transport the very fine suspended sediment modes and current maxima occur simultaneously with the observed Population I "High" occurrences near the bottom. Towards the end of the time-series (after 26 September) a longer peak of the Crestuma Dam discharge seems to have an effect on the quantity of available sediment at the Barra deployment site. After this date, Population I "High" signatures are present in the water column at the end of ebb, and then near the bottom in the beginning of flood, mimicking the already described conceptual cyclical model.

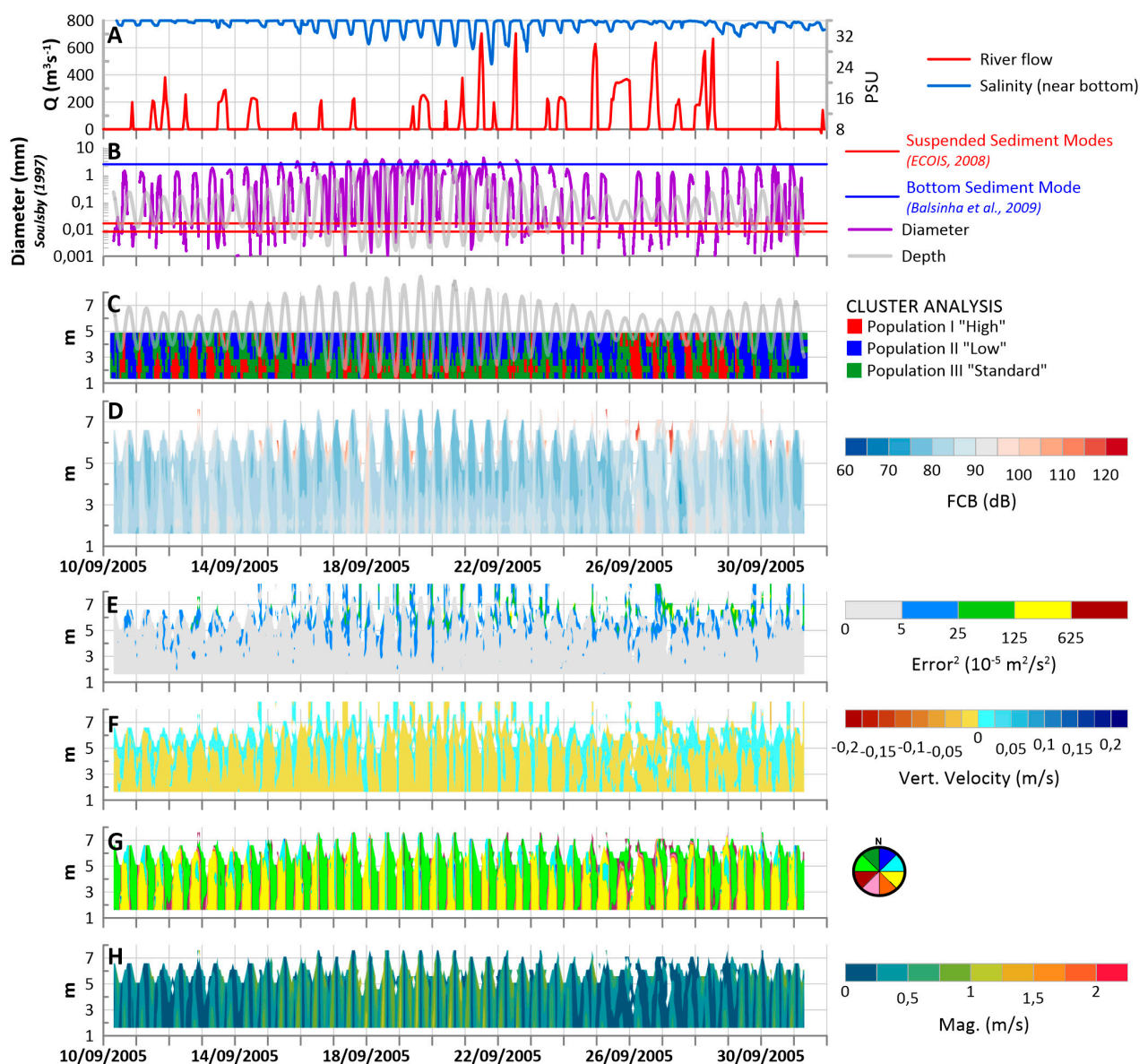


Figure 3. Douro 2005 “Barra” dataset. (A) Douro river flow measured at Crestuma Dam and near bottom salinity measured at the bottom mounted RCM9; (B) Potentially removable/transportable particle size [30] and known bottom sediment and suspended sediment main modes [22,35]; (C) K-means cluster analysis of $z_{score}(FCB)$ superimposed on ADCP transducer depth (tide); (D) Fluid Corrected backscatter (FCB); (E) error velocity squared (proxy of turbulent kinetic energy); (F) Vertical velocity; (G) Current direction; (H) Horizontal velocity (current magnitude).

3.2. Winter of 2007

Minho river flow records measured at Foz de Mouro during the winter of 2007 observation period reveal an artificial daily pattern imposed by the Frieira Dam discharges. Dam discharges occur after 12:00 everyday up to approximately 0:00 of the next day (12 h) with a small interruption at about 18:00. As a result, discharge values as high as 600–800 m³/s and as low 100 m³/s were felt during the Minho Barra 2007 deployment period (Figure 4H). The general increase of fresh water contribution during winter conditions at the Barra measuring position is reflected in the significantly lower salinity values when compared to summer/low runoff conditions. Salinities reveal the presence of brackish water at the Barra position, oscillating between 8 and 16 PSU with the semi-diurnal tide. This oscillation is not affected by the varying river runoff measured at Foz de Mouro (Figure 4H). ADCP records show a clear tidal evolution of the $z_{score}(FCB)$ cluster/suspended particle populations.

Population I “High” takes up most of the water column during ebb, low-tide and flood concentrating at near bottom levels and subsiding into Population III “Standard” towards the surface. Population II “Low” is present during high-tide, confirming that under these typical winter river discharge forcing conditions, suspended particle source at the lower end of the Minho estuary is clearly the fluvial/estuarine input (Figure 4F). Soulsby’s (1997) removable sediment formulations show that bottom sediment main modes are potentially mobilized by tidal currents during most of the tidal cycle, with the exception of ebb and flood slacks, and current direction shows that the current has a general downstream direction during most of the tidal cycle, with the exception of the last part of flood (Figure 4G,C). Although in the summer of 2005, a tidal asymmetry was identified with stronger shorter floods and longer weaker ebbs, during this observation period, ebb currents are stronger and longer than floods, reinforced by the higher river discharges and available turbulence seems to be lower than in 2005, when this part of the estuary was clearly only dominated by the tidal forcing.

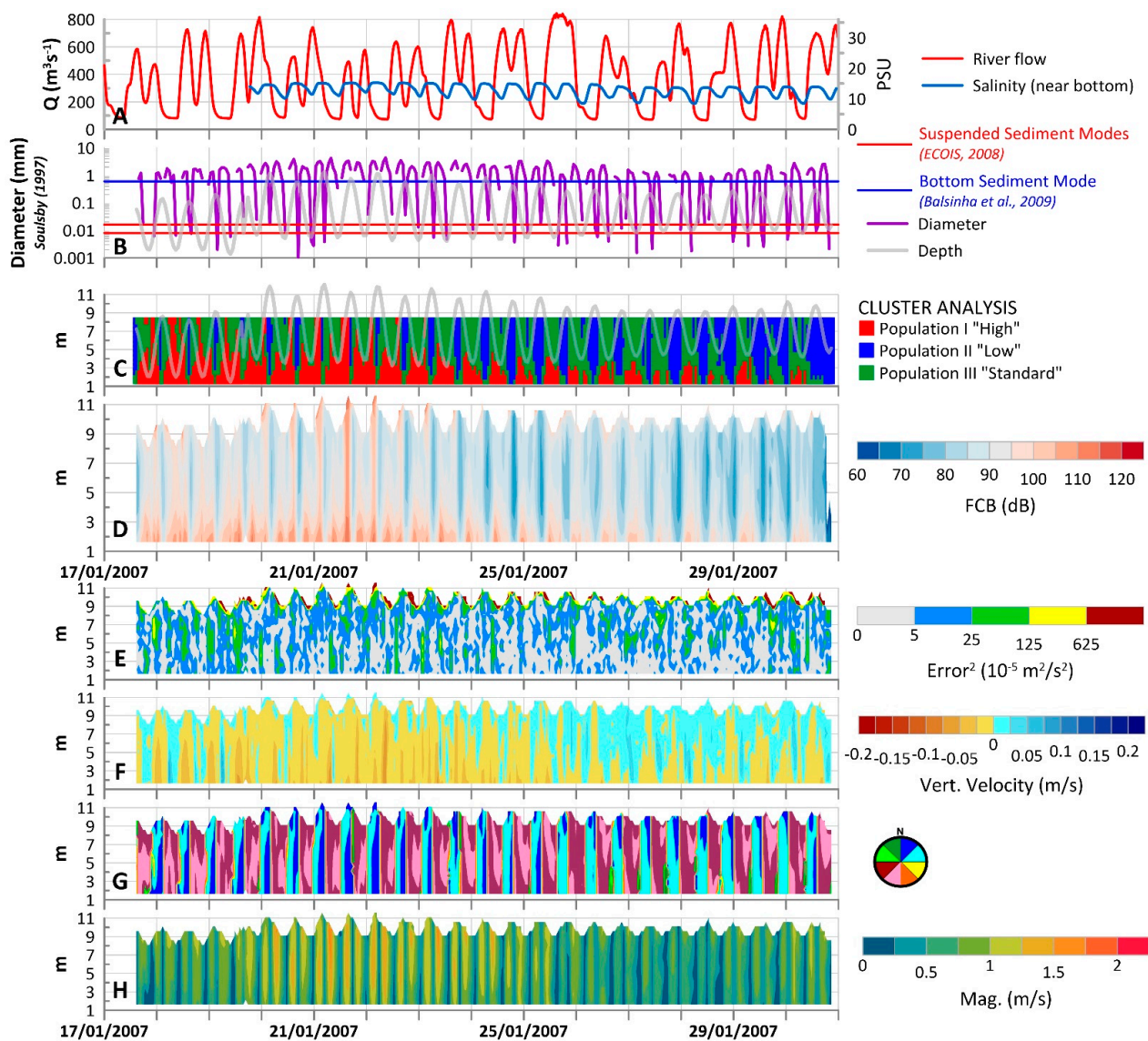


Figure 4. Minho 2007 “Barra” dataset. (A) Minho river flow measured at Foz de Mouro and near bottom salinity measured at the bottom mounted RCM9; (B) Potentially removable/transportable particle size [30] and known bottom sediment and suspended sediment main modes [22,35]; (C) K-means cluster analysis of $z_{score}(FCB)$ superimposed on ADCP transducer depth (tide); (D) Fluid Corrected backscatter (FCB); (E) error velocity squared (proxy of turbulent kinetic energy); (F) Vertical velocity; (G) Current direction; (H) Horizontal velocity (current magnitude).

In Part 1, a sediment export estimate of approximately 10^5 kg per semi-diurnal tidal cycle was presented, calculated for the ECOIS winter of 2006 survey, which was carried out under river discharge values in the same order of magnitude as the ones registered during the 2007 observation period (300 to 500 m^3/s mean daily discharge at Foz de Mouro), so it is plausible to assume that the same order of magnitude of sediment export could be inferred for this observation period. It is also possible to admit, under the observed forcing scenario, that the Minho Estuary is capable of exporting coarse material present in the estuary's water column, as a result of bottom remobilization and transport, since most of the $z_{\text{score}}(\text{FCB})$ maxima are found near the bottom, suggesting the presence of higher concentrations of sands eventually finding their way into the inner shelf.

In the Douro estuary, Crestuma Dam discharge data shows two distinct forcing scenarios during the winter 2007 measuring period. From the beginning of the time series (20 January) up to 11 February, river discharges reveal artificially regulated values varying from 0 up to 1500 m^3/s . After this date, river discharges significantly increase to continuous values over 1500 m^3/s , with maxima of ≈ 2500 m^3/s . Near bottom temperatures (no valid salinity measurements were available for this observation period), oscillate with tide, revealing a significant cooler estuarine contribution, very evident after 11 February (Figure 5H).

In the first period (20 January 20 up to 11 February), current magnitudes vary with the tidal fluxes and amplitude, with maxima associated with ebbs and floods during spring tide periods and decreasing during neaps (Figure 5B,C). Cluster partitioning identifies Population I ("High") during ebbs when these coincide with peaks of river discharge (Figure 5A), Population II ("Low") typifies some spring and most of neap floods and Population III ("Standard") is typical of neap tide ebbs and spring tide flood slacks (Figure 5F).

After 11 February, flooding in the estuary changes the sediment dynamics scenario dramatically. Current magnitudes reach maxima of 1.2 m/s and are permanently directed downstream, with the estuary temporarily transformed into a river. The combined effect of the increase in river discharge values and neaps significantly diminishes the marine influence at this point of the estuary and cluster populations show the dominance of Population I ("High") and the almost absence of the "Low" Population II (Figure 5F). As the tidal amplitude increases after 14 February 14, Population I "High" is replaced by Population III "Standard" during floods.

Under this hydrodynamic setting the Douro outlet flow is able to transport the finer particles in suspension during most of the analyzed mooring period. However, the flow is only able to transport the locally found sand bottom sediment during peak discharge conditions combined with ebbs. If the characterization of the suspended sediment signatures established in Santos et al. (2021) [21] is taken into consideration, Population I ("High") is representative of finer material of fluvial origin which might or might not be aggregated into flocs transported from upstream to the deployment site, since it is generally found when the fluvial discharge values peak and not necessarily when the current magnitudes are high. As far as Population II ("Low") is concerned, it is representative of flood maxima and flood slacks during spring tides, synchronous with the higher influence of marine waters at this point of the estuary, and it is representative of most of the semi-diurnal tidal period during neaps, when river discharges are under 1000 m^3/s . Data seems to reveal that the lower acoustic responses that yielded the identification of Population II may be due to the lowering concentration (due to the formation of flocs and consequent deposition in the presence of higher salinities) or local deposition of essentially fine particles transported from upstream during tidal slacks. Given this interpretation, the characterization of $z_{\text{score}}(\text{FCB})$ clusters as Population III ("Standard") is attributed to lower concentrations events of the same type of particles that make up Population I ("High"). As an example, after 2 days of river discharges ≈ 1500 m^3/s on 13 and 14 February, the upstream flow starts to be counteracted by the increasing tidal amplitude during flood, leading to a decrease in the current magnitude and fluvial water's input at this point of the estuary. At this time,

ADCP clusters transition from Population I to Population III, especially during floods, when the influence of the fluvial discharge is temporarily weakened by the flood entrance.

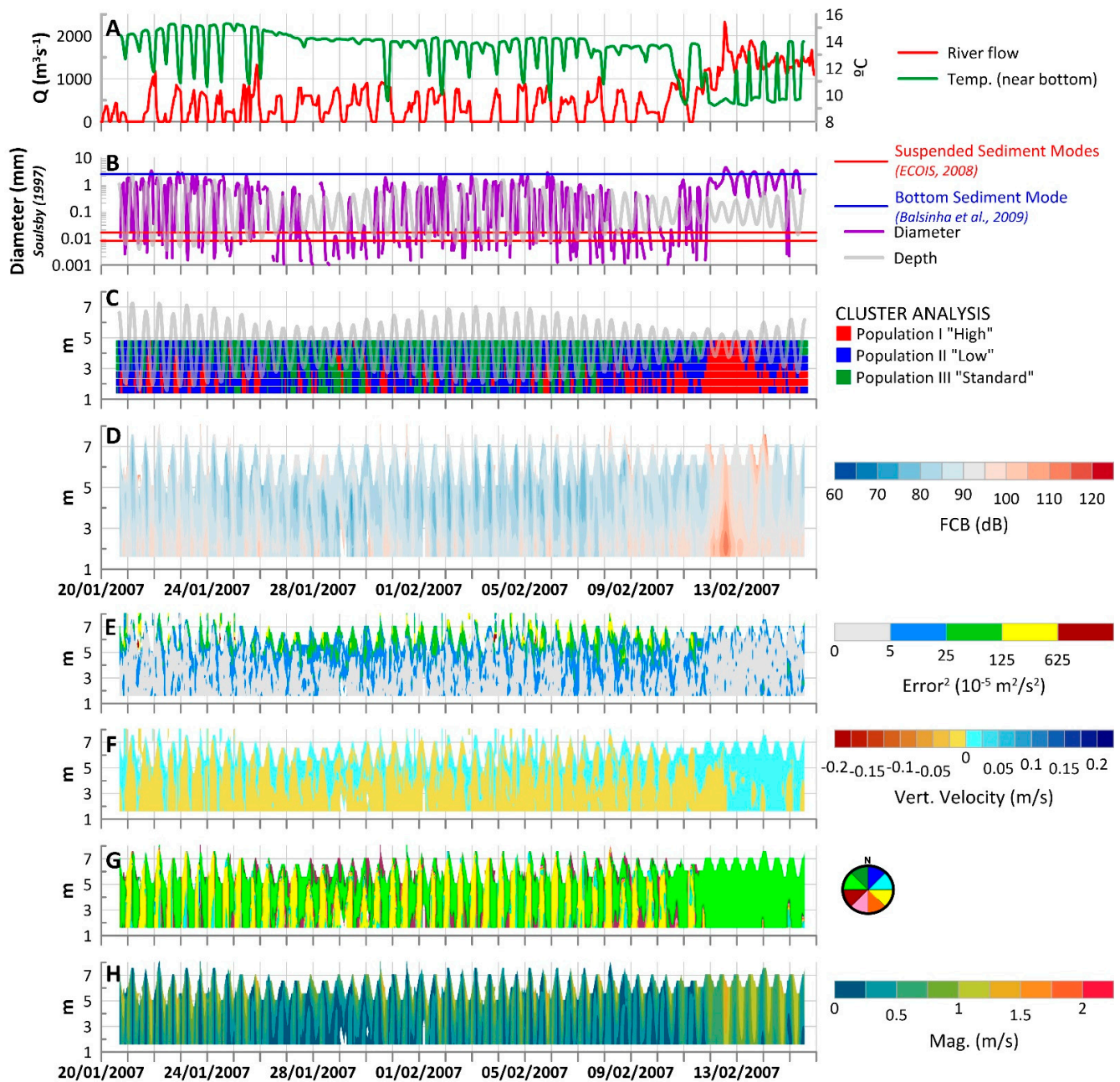


Figure 5. Douro 2007 “Barra” dataset. (A) Douro river flow measured at Crestuma Dam and near bottom temperature measured at the bottom mounted RCM9; (B) Potentially removable/transportable particle size [30] and known bottom sediment and suspended sediment main modes [22,35]; (C) K-means cluster analysis of $z_{score}(FCB)$ superimposed on ADCP transducer depth (tide); (D) Fluid Corrected backscatter (FCB); (E) error velocity squared (proxy of turbulent kinetic energy); (F) Vertical velocity; (G) Current direction; (H) Horizontal velocity (current magnitude).

4. Discussion and Final Considerations

In this work, single frequency ADCP monitoring data collected in two contrasting seasonal scenarios inside the Douro and Minho estuaries was used to establish the general hydrodynamic and sediment transport patterns in both water columns. Datasets were collected in the summer of 2005, during an exceptionally dry hydrological year and winter

of 2007, when both the Minho and Douro basins were recovering from a two-year stretch of drought.

The application of k-means cluster analysis to the normalized fluid corrected backscatter time-series allowed for a clear identification of the time and water column intervals populated by different suspended particle signatures, mostly in terms of concentration. The inference of different types of particle size distributions, in the case of this work, is hampered by the lack of in-situ measurements of PSD which would allow a better interpretation of the ADCP response, as was the case in Santos et al. (2021). In most of the datasets analyzed by these authors, it was found that ADCP $z_{score}(FCB)$ responds equally as strong to increasing particle concentration as to increase in the fine sediment ($<62.5 \mu\text{m}$) relative frequency, so it is possible that in the case of the discussed ECOIS datasets, the ADCP might exacerbate its response to the presence of fine material in the ensonified column [18,21]. Additionally, we are not able to distinguish if this fine material is present in flocculated or as individual particles since the ADCP's response is, according to the findings of [22], consistent with the scattering of the tightly bound primary fine particles as opposed to the larger flocs [23]. However, the general understanding of estuarine sediment dynamics, the limited available information about both bottom sediments present at the mooring sites and suspended sediments present in the estuaries' water column, as well as the forcing conditions recorded by the ADCP itself, allowed for a plausible identification of the type of particles that constitute each of the identified $z_{score}(FCB)$ populations [22,35–37].

Although the Douro estuary is generally recognized by most authors as the main source of sediment in the NW Iberian inner shelf/coastal system, no evidence of coarse material export from this estuary into the inner shelf could be inferred from the ECOIS ADCP datasets presented in this work or in Part 1 of this same study. During these periods, sediment transport patterns inside the lower Douro estuary were characterized by the tidal cyclical upstream/downstream transport of mostly fine material of fluvial/estuarine origin, which in some calmer periods might flocculate and settle at the lower reaches of the estuary, yielding a net import of sediments under low river runoff and a near negligible export of sediments during high river runoff springs (see Part 1 of this study). Net sediment export from the Douro estuary into the inner shelf was observed during high river runoff neaps, when the energy imposed by the lower tidal amplitude was not sufficient to counteract the river flow. However, the interpretation of the observed $z_{score}(FCB)$ clusters and the fact that, even during intervals of extreme river runoff ($>1500 \text{ m}^3/\text{s}$), currents recorded at the estuary's lower end are unable to transport resident coarse bottom material, leads to the conclusion that this exported material was generally composed of fine low density particles of fluvial/terrestrial origin, not the kind of material that will eventually nourish the littoral.

Minho estuarine dynamics, as observed in the ECOIS 2005 and 2007 ADCP datasets is clearly dominated by the tide. The discussed observations confirm the findings of ECOIS team (2008) and Part 1 of this study, which describe the Minho estuary as vertically homogeneous as far as the current structure is concerned during both spring and neaps [22]. In the Minho estuary, where estuarine morphology is characterized by its shallow depths and numerous sand banks, the energy imposed by the tidal currents is able to actively homogenize the whole water column. When compared to the Douro datasets, the ADCP datasets recorded in the Minho revealed higher levels of turbulence and vertical velocities associated with tidal fluxes, resulting in an effective mixing of the water column structure. During the summer (2005) no evidence of effective sediment transport into the inner shelf could be inferred from the Barra dataset. At the estuary's outlet, two different origin suspended sediment populations floated in and out of the estuary as the tide fluctuated: one concentrated near the bottom, probably as result of sandy bottom sediment remobilization, and a second one floating into the estuary at surface levels revealing a low-density nature, but with a clear marine origin. This sediment dynamics pattern confirms the results presented in Part 1, which determined a net import of sediment into the estuary during a spring tide semi-diurnal tidal cycle, probably made up of sandy near bottom transported

material, and a close to null export during neaps. During the wet 2007 winter however, this scenario changes. The significant increase of the river flow reinforces the generally weaker and longer ebbs, which gain enough energy to remobilize the sandy material accumulated at the estuary bottom and effectively export it to the inner shelf where it eventually may nourish the southern littoral zone.

In their work, Ponte Lira et al. (2016) presented coastline evolution rates for the low stand sandy Portuguese coast estimated from 1958 up to the present [4]. This study shows a clear retreat of the coastline just south of the Douro estuary, as a result of the known sediment deficit. However, just south of the Minho estuary, there is evidence of the coastline's equilibrium and in some cases even advance, showing that the low artificialization (when compared to the Douro) of the Minho lower estuary is still able to somehow preserve the natural sediment budget in the Portuguese northernmost coastal cell.

In short, this work's results confirm the already known present scarcity of (sandy) sediment export from the Douro and Minho estuaries into the inner shelf and the consequent sediment depletion of the adjacent littoral. No effective contribution of the Douro to this budget could be inferred from the analyzed datasets, but evidence of sand export was observed from the Minho outlet during the winter of 2007, showing that for the analyzed periods the Minho outflow is a significant source of sediment supply to the near coastal zone.

Author Contributions: Conceptualization, A.I.S. and D.C.; Methodology, A.I.S. and A.O.; Project administration, A.O.; Software, A.I.S.; Supervision, J.P.P. and M.C.F.; Validation, D.C.; Writing—original draft, A.I.S.; Writing—review & editing, A.O., D.C., J.P.P. and M.C.F. All authors have read and agreed to the published version of the manuscript.

Funding: This particular research received no external funding.

Institutional Review Board Statement: Not Applicable.

Informed Consent Statement: Not applicable.

Data Availability Statement: ECOIS datasets are available upon request at geral@hidrografico.pt. River flow data for the Foz de Mouro and Crestuma-Lever Dam was retrieved from the Portuguese Environmental Agency portal: Sistema Nacional de Informação de Recursos Hídricos, available at <http://snirh.apambiente.pt/> (Agência Portuguesa do Ambiente).

Acknowledgments: Projects ECOIS and NICC were financed by the Portuguese Ministry of Science and Technology with the references POCTI/CTA/48461/2002 (ECOIS) and POCTI/CTA/49563/2002 (NICC) between 2005 and 2008. No part of this work would be possible without the invaluable contributions of everyone in the ECOIS team. Special appreciation is due to the colleagues A. Jorge da Silva and Maria João Balsinha Fernandes who are moral co-authors of this work. Minho Flow values after 2008 up to April 2015 were kindly provided by the Spanish authorities (Centro Cuenca SAIH Miño-Sil) for values measured in the Frieira Dam.

Conflicts of Interest: The authors declare no conflict of interest.

References

1. Alveirinho Dias, J.M.; Boski, T.; Rodrigues, A.; Magalhães, F. Coast Line Evolution in Portugal since the Last Glacial Maximum until Present—A Synthesis. *Mar. Geol.* **2000**, *170*, 177–186. [CrossRef]
2. Andrade, C.F. *Dinâmica Erosão e Conservação Das Zonas de Praia*; Parque EXPO 98: Lisbon, Portugal, 1997; ISBN 972 8396 75 9.
3. Duarte Santos, F.; Mota Lopes, A.; Moniz, G.; Ramos, L.; Taborda, R. *Grupo de Trabalho Do Litoral: Gestão Da Zona Costeira: O Desafio Da Mudança*; Duarte Santos, F., Penha-Lopes, G., Mota Lopes, A., Eds.; Lisbon, Portugal, 2017; ISBN 978-989-99962-1-2.
4. Ponte Lira, C.; Nobre Silva, A.; Taborda, R.; Freire de Andrade, C. Coastline Evolution of Portuguese Low-Lying Sandy Coast in the Last 50 Years: An Integrated Approach. *Earth Syst. Sci. Data* **2016**, *8*, 265–278. [CrossRef]
5. Santos, A.I.; Oliveira, A.; Pinto, J.P.; Freitas, M.C. Hydrodynamic and Sediment Transport Patterns in the Minho and Douro Estuaries (NW Portugal) Based on ADCP Monitoring Data: Part 1—Tidal Sediment Exchanges. *Coasts* **2021**, *1*, 3. [CrossRef]
6. Oliveira, A.; Santos, A.I.; Morgado, A.; Jorge da Silva, A. Suspended Sediment Mineralogical Signature—An Approach to Understand Shelf Water Hydrodynamics. In Proceedings of the PECS 2008: Physics of Estuaries and Coastal Seas, Liverpool, UK, 25–29 August 2008.
7. Alveirinho Dias, J.M.; Jouanneau, J.M.; Gonzalez, R.; Araújo, M.F.; Drago, T.; Garcia, C.; Oliveira, A.; Rodrigues, A.; Vitorino, J.; Weber, O. Present Day Sedimentary Processes on the Northern Iberian Shelf. *Prog. Oceanogr.* **2002**, *52*, 249–259. [CrossRef]

8. Libicki, C.; Bedford, K.W.; Lynch, J.F. The Interpretation and Evaluation of a 3-MHz Acoustic Backscatter Device for Measuring Benthic Boundary Layer Sediment Dynamics. *J. Acoust. Soc. Am.* **1989**, *85*, 1501–1511. [[CrossRef](#)]
9. Hanes, D.M.; Vincent, C.E.; Huntley, D.A.; Clarke, T.L. Acoustic Measurements of Suspended Sand Concentration in the C₂S₂ Experiment at Stanhope Lane, Prince Edward Island. *Mar. Geol.* **1988**, *81*, 185–196. [[CrossRef](#)]
10. Hay, A.E. On the Remote Acoustic Detection of Suspended Sediment at Long Wavelengths. *J. Geophys. Res.* **1983**, *88*, 7525–7542. [[CrossRef](#)]
11. Gartner, J.W. Estimating Suspended Solids Concentrations from Backscatter Intensity Measured by Acoustic Doppler Current Profiler in San Francisco Bay, California. *Mar. Geol.* **2004**, *211*, 169–187. [[CrossRef](#)]
12. Hoitink, A.J.F.; Hoekstra, P. Observations of Suspended Sediment from ADCP and OBS Measurements in a Mud-Dominated Environment. *Coast. Eng.* **2005**, *52*, 103–118. [[CrossRef](#)]
13. Guerrero, M.; Rütther, N.; Szupiany, R.; Haun, S.; Baranya, S.; Latosinski, F. The Acoustic Properties of Suspended Sediment in Large Rivers: Consequences on ADCP Methods Applicability. *Water* **2016**, *8*, 13. [[CrossRef](#)]
14. Latosinski, F.G.; Szupiany, R.N.; García, C.M.; Guerrero, M.; Amsler, M.L. Estimation of Concentration and Load of Suspended Bed Sediment in a Large River by Means of Acoustic Doppler Technology. *J. Hydraul. Eng.* **2014**, *140*, 04014023. [[CrossRef](#)]
15. Moore, S.A.; Le Coz, J.; Hurther, D.; Paquier, A. Using Multi-Frequency Acoustic Attenuation to Monitor Grain Size and Concentration of Suspended Sediment in Rivers. *J. Acoust. Soc. Am.* **2013**, *133*, 1959–1970. [[CrossRef](#)]
16. Topping, D.J.; Wright, S.A.; Melis, T.S.; Rubin, D.M. High-Resolution Measurements of Suspended-Sediment Concentration and Grain Size in the Colorado River in Grand Canyon Using a Multi-Frequency Acoustic System. In Proceedings of the 10th International Symposium on River Sedimentation, World Association for Sediment and Erosion Research, Moscow, Russia, 1–4 August 2007; Volume 3, p. 19.
17. Wright, S.A.; Topping, D.J.; Williams, C.A. Discriminating Silt-and-Clay from Suspended-Sand in Rivers Using Side-Looking Acoustic Profilers. In Proceedings of the 2nd Joint Federal Interagency Conference, Las Vegas, NV, USA, 27 June–1 July 2010; p. 12. [[CrossRef](#)]
18. Santos, A.I.; Oliveira, A.; Carinhas, D.; Pinto, J.P.; Zacarias, N.; Freitas, M.C. The Acoustic Properties of In-Situ Measured Suspended Sediments and Their Implications on Concurrent ADCP Response—Case Studies of the Portuguese Inner Shelf. *Mar. Geol.* **2020**, *419*. [[CrossRef](#)]
19. Agrawal, Y.C.; Pottsmith, H.C. Instruments for Particle Size and Settling Velocity Observations in Sediment Transport. *Mar. Geol.* **2000**, *168*, 89–114. [[CrossRef](#)]
20. Agrawal, Y.C.; Whitmire, A.; Mikkelsen, O.A.; Pottsmith, H.C. Light Scattering by Random Shaped Particles and Consequences on Measuring Suspended Sediments by Laser Diffraction. *J. Geophys. Res. Ocean.* **2008**, *113*, 1–11. [[CrossRef](#)]
21. Santos, A.I.; Carinhas, D.; Oliveira, A.; Pinto, J.P.; Freitas, M.C.; Hanes, D.M. A Statistical Interpretation of Acoustic Backscatter and Laser Responses to Suspended Particle Variations in the Coastal Shelf. *Mar. Geol.* **2021**, *436*, 106474. [[CrossRef](#)]
22. ECOIS Team. *ECOIS-Estuarine Contributions on Inner Shelf Dynamics (POCTI/CTA/48461/2002). Relatório Final*; FCT—Fundação para a Ciência e Tecnologia: Lisboa, Portugal, 2008.
23. Vincent, C.E.; MacDonald, I.T. A Flocculi Model for the Acoustic Scattering from Floccs. *Cont. Shelf Res.* **2015**, *104*, 15–24. [[CrossRef](#)]
24. MacDonald, I.T.; Vincent, C.E.; Thorne, P.D.; Moate, B.D. Acoustic Scattering from a Suspension of Flocculated Sediments. *J. Geophys. Res. Ocean.* **2013**, *118*, 2581–2594. [[CrossRef](#)]
25. Thorne, P.D.; Hurther, D. An Overview on the Use of Backscattered Sound for Measuring Suspended Particle Size and Concentration Profiles in Non-Cohesive Inorganic Sediment Transport Studies. *Cont. Shelf Res.* **2014**, *73*, 97–118. [[CrossRef](#)]
26. Lee, T.H.; Hanes, D.M. Direct Inversion Method to Measure the Concentration Profile of Suspended Particles Using Backscattered Sound. *J. Geophys. Res.* **1995**, *100*, 2649. [[CrossRef](#)]
27. Venditti, J.G.; Church, M.; Attard, M.E.; Haught, D. Use of ADCPs for Suspended Sediment Transport Monitoring: An Empirical Approach. *Water Resour. Res.* **2016**, *52*, 2715–2736. [[CrossRef](#)]
28. Gostiaux, L.; van Haren, H. Extracting Meaningful Information from Uncalibrated Backscattered Echo Intensity Data. *J. Atmos. Ocean. Technol.* **2010**, *27*, 943–949. [[CrossRef](#)]
29. Gordon, R.L. *Acoustic Doppler Current Profiler Principles of Operation—A Practical Primer*; RD Instruments: San Diego, CA, USA, 1996; p. 52.
30. Soulsby, R.L. *Dynamics of Marine Sands: A Manual for Practical Applications*; Thomas Telford Publications: London, UK, 1997.
31. Agência Portuguesa do Ambiente Sistema Nacional de Informação de Recursos Hídricos. Available online: <https://snirh.apambiente.pt/> (accessed on 18 November 2021).
32. Confederación Hidrográfica Miño-Sil CHMiñoSil—Confederación Hidrográfica Miño-Sil. Available online: <https://www.chminosil.es/es/> (accessed on 18 November 2021).
33. Vieira, M.E.C.; Bordalo, A.A. The Douro Estuary (Portugal): A Mesotidal Salt Wedge. *Oceanol. Acta* **2000**, *23*, 585–594. [[CrossRef](#)]
34. Reis, J. *Caracterização Da Maré No Estuário Do Minho*; Instituto Superior Técnico—Universidade Técnica de Lisbon: Lisbon, Portugal, 2008.
35. Balsinha, M.J.; Santos, A.I.; Alves, A.M.; Oliveira, A.T. Textural Composition of Sediments from Minho and Douro Estuaries (Portugal) and Its Relation with Hydrodynamics. *J. Coast. Res.* **2009**, *56*, 1330–1334. [[CrossRef](#)]
36. Portela, L.I. Sediment Transport and Morphodynamics of the Douro River Estuary. *Geo-Mar. Lett.* **2008**, *28*, 77–86. [[CrossRef](#)]
37. Instituto Hidrográfico. *Campanha Hidro-Morfológica Para o Estudo Da Barra Do Douro—Trabalho Realizado a Pedido Da APDL—SET/OUT 1994*; Instituto Hidrográfico: Lisboa, Portugal, 1995.